

# Capture theory models: An overview of their development, experimental verification, and applications to ion-molecule reactions F

Cite as: J. Chem. Phys. **157**, 060901 (2022); <https://doi.org/10.1063/5.0098552>

Submitted: 10 May 2022 • Accepted: 10 June 2022 • Accepted Manuscript Online: 23 June 2022 • Published Online: 08 August 2022

Andriana Tsikritea,  Jake A. Diprose,  Timothy P. Softley, et al.

## COLLECTIONS

F This paper was selected as Featured



View Online



Export Citation



CrossMark

## ARTICLES YOU MAY BE INTERESTED IN

[On the nature of the chemical bond in valence bond theory](#)

The Journal of Chemical Physics **157**, 090901 (2022); <https://doi.org/10.1063/5.0095953>

[Design and characterization of a cryogenic linear Paul ion trap for ion-neutral reaction studies](#)

Review of Scientific Instruments **93**, 033201 (2022); <https://doi.org/10.1063/5.0080458>

[Density-functional theory vs density-functional fits](#)

The Journal of Chemical Physics **156**, 214101 (2022); <https://doi.org/10.1063/5.0091198>



Time to get excited.  
Lock-in Amplifiers – from DC to 8.5 GHz

Find out more

Zurich Instruments

# Capture theory models: An overview of their development, experimental verification, and applications to ion–molecule reactions

Cite as: *J. Chem. Phys.* **157**, 060901 (2022); doi: [10.1063/5.0098552](https://doi.org/10.1063/5.0098552)

Submitted: 10 May 2022 • Accepted: 10 June 2022 •

Published Online: 8 August 2022



View Online



Export Citation



CrossMark

Andriana Tsikritea,<sup>1</sup> Jake A. Diprose,<sup>1</sup>  Timothy P. Softley,<sup>2</sup>  and Brianna R. Heazlewood<sup>1,a)</sup> 

## AFFILIATIONS

<sup>1</sup>Department of Physics, University of Liverpool, Liverpool L69 7ZE, United Kingdom

<sup>2</sup>School of Chemistry, University of Birmingham, Edgbaston B15 2TT, United Kingdom

<sup>a)</sup>Author to whom correspondence should be addressed: [b.r.heazlewood@liverpool.ac.uk](mailto:b.r.heazlewood@liverpool.ac.uk)

## ABSTRACT

Since Arrhenius first proposed an equation to account for the behavior of thermally activated reactions in 1889, significant progress has been made in our understanding of chemical reactivity. A number of capture theory models have been developed over the past several decades to predict the rate coefficients for reactions between ions and molecules—ranging from the Langevin equation (for reactions between ions and non-polar molecules) to more recent fully quantum theories (for reactions at ultracold temperatures). A number of different capture theory methods are discussed, with the key assumptions underpinning each approach clearly set out. The strengths and limitations of these capture theory methods are examined through detailed comparisons between low-temperature experimental measurements and capture theory predictions. Guidance is provided on the selection of an appropriate capture theory method for a given class of ion–molecule reaction and set of experimental conditions—identifying when a capture-based model is likely to provide an accurate prediction. Finally, the impact of capture theories on fields such as astrochemical modeling is noted, with some potential future directions of capture-based approaches outlined.

© 2022 Author(s). All article content, except where otherwise noted, is licensed under a Creative Commons Attribution (CC BY) license (<http://creativecommons.org/licenses/by/4.0/>). <https://doi.org/10.1063/5.0098552>

## I. INTRODUCTION

There has long been a desire to understand how chemical reactions occur on a fundamental level. In order to accurately model and predict the behavior of complex gas-phase environments—such as the chemistry occurring in the atmosphere, in the interstellar medium, and in combustion engines—we need to understand the properties of the individual competing reactions that can occur within these settings. Almost 150 years ago, Arrhenius proposed an equation to describe the behavior of thermally activated reactions (based on the earlier observations of van't Hoff), where reactants need to surpass an energy barrier before proceeding to products.<sup>1</sup> When more energy is available to the system, the Arrhenius equation predicts that the probability of a reaction occurring is increased. While the Arrhenius equation (and the transition-state and collision theories developed to explain it) is a powerful predictive tool for many classes of reactions, it is not valid when the reaction partners experience a strong attraction at long range—an interaction that

commonly occurs in collisions between an ion and a neutral species. This is because, in many ion–neutral reaction systems, the process is dominated by the strong long-range attractive forces between the reactants and there is no energetic barrier to reaction (see Fig. 1).

Reactions between ions and neutral molecules are known to be important in many naturally occurring low-temperature gas-phase environments. Ion–molecule reactions can exhibit high rate coefficients at low temperatures—in many cases, proceeding faster as the temperature falls, while at the same time many other competing processes effectively stop altogether. To better describe the behavior of ion–neutral reaction processes, a number of methods were developed in which the rate of reaction is determined by the rate of ‘capture’ of the reactant pairs into a state of molecular association—in an attractive potential energy well—from which reaction is assumed to proceed with unit probability. In some simple molecular systems, this may be a short-lived, transient state through which the system passes directly on its way to products. In other cases, a long-lived complex may be formed—for example, the system

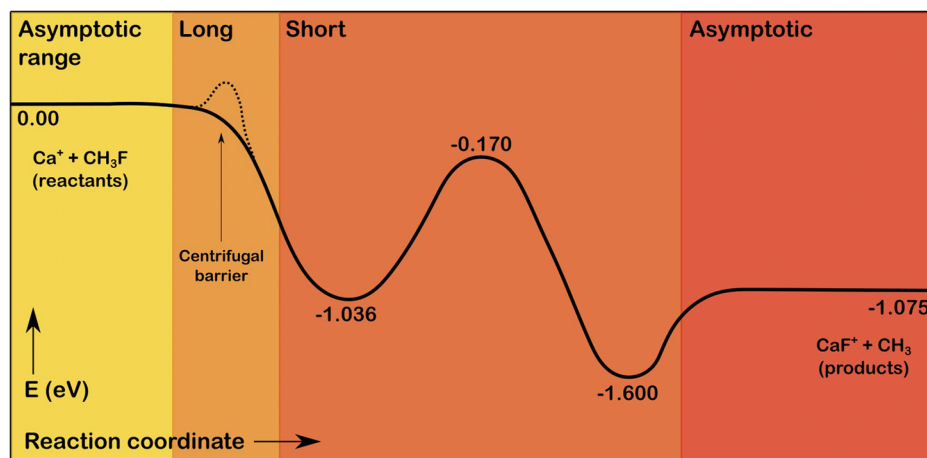


**FIG. 1.** Schematic depiction of the barrierless, exothermic reaction between the ground-state  $\text{Ca}^+(^2S_{1/2})$  ions and neutral  $\text{CH}_3\text{F}$  molecules, adapted from Ref. 2. The reaction coordinate is divided into different regions, indicating where the long-range and short-range forces are dominant. A dashed centrifugal barrier can be seen in the long-range potential, with a submerged barrier present in the short-range region. Energies are reported (in eV) with respect to the entrance of the  $\text{Ca}^+ + \text{CH}_3\text{F}$  channel.

can be trapped behind a submerged barrier on the path to product formation (see Fig. 1). In either case, the assumption of capture theory is that, once formed in this associated state, the system is captured for reaction and has a zero probability of reverting back to the reactant species.

First introduced in the 1970s and 1980s, capture theory methods were designed to describe the ‘barrierless’ processes that the Arrhenius equation could not account for by explicitly considering the strong long-range attractive forces between reactants. In this way, the interaction potential can be expressed as an expansion series of the distance  $R$  between the colliding particles,

$$V_R = \sum_n -\frac{C_n}{R^n}. \quad (1)$$

The leading power  $n$ , as well as the interaction coefficient  $C_n$  for a given reaction system, depends on the nature of the interaction; several of the most common types of ion–neutral interactions are summarized in Table I.

For collisions that are not head-on [i.e., when the reactants approach each other with a non-zero impact parameter (see Fig. 2)], a centrifugal term needs to be added to the potential to account for the relative orbital motion of the colliding particles. An effective potential of the form

$$V_{\text{eff}} = \frac{l^2}{2\mu R^2} - \sum_n \frac{C_n}{R^n} \quad (2)$$

**TABLE I.** Common types of interactions found in ion–neutral reaction systems, with  $\mu_D$  the dipole moment of the neutral reactant (for polar species),  $\theta$  the angle between the vector of the ion–neutral separation and the molecular axis,  $Q$  the quadrupole moment of the neutral, and  $\alpha$  the polarizability of the neutral species.

Interaction	$n$	$C_n$
Ion–dipole	2	$\mu_D \cos(\theta)$
Ion–quadrupole	3	$-Q(3\cos^2(\theta) - 1)/2$
Ion–induced dipole	4	$\alpha/2$

can be written, with the angular momentum ( $l$ ) defined as

$$l = \mu vb, \quad (3)$$

where  $\mu$  is the reduced mass of the system,  $v$  the relative velocity of the colliding species, and  $b$  the impact parameter. The first term of Eq. (2) adds a barrier to the (otherwise barrierless) potential: the so-called centrifugal barrier (see Fig. 2). Note that although the simplest capture theories assume that  $l$  is a continuous variable, this is actually a quantized parameter of the collision, hence the depiction in Fig. 2 of  $l = 0, 1, \dots$  effective potential curves.

Central to all capture theory methods is the assumption that a collision event will yield products with unit probability, provided the reactants have enough energy to surmount the centrifugal barrier. The rates of ion–neutral reaction systems often display an inverse trend with temperature, with enhanced rates at low temperatures. As will be discussed below, capture theory methods can predict this behavior.<sup>4,5</sup> A key benefit of many of the early capture theory methods is their simplicity and ease of use; armed with only a few key details about the reaction system—such as the masses, multipole moments, and polarizabilities—one can straightforwardly calculate the capture-based rate coefficient. The relative ease with which rate coefficients can be estimated using capture theory methods has seen them widely adopted—to provide a comparison to experimental findings, to help explain the behavior of a given reaction system, and in place of experimental measurements where there is limited data. For example, capture theory plays an important role in predicting the rate coefficients of many important astrochemical processes for which there is no reliable experimental data at the relevant low temperatures. However, the simplicity of many capture theory methods also gives rise to limitations.

A drawback of capture theory approaches is that they do not account for interactions that happen at short range (i.e., when the collision partners are close to one another). This arises because capture theories consider only the likelihood that two reactants form a reaction complex, based on their long-range attraction. As such, capture theories cannot identify what products might be formed or predict the branching ratios of different reaction pathways when more than one product channel is available. Intrinsic features of the

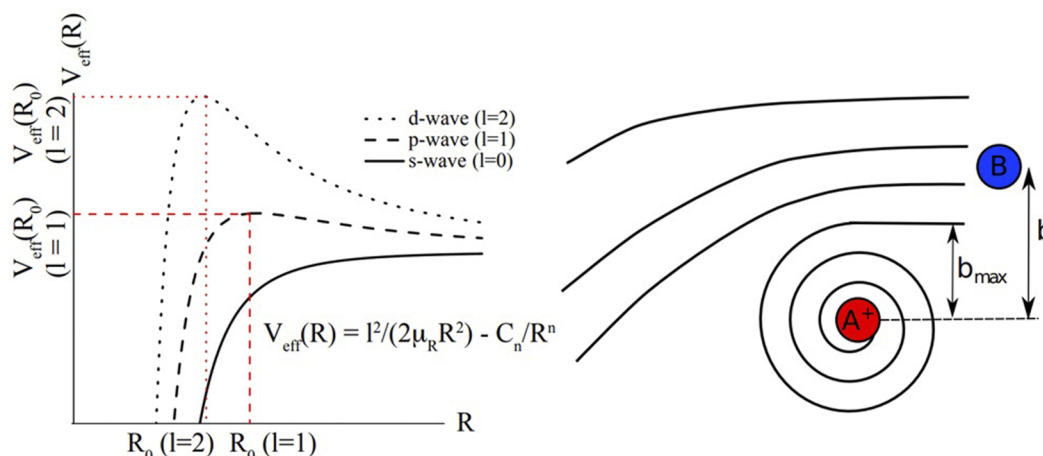


**FIG. 2.** Left: plot of the effective interaction potential,  $V_{\text{eff}}(R)$ , as a function of the separation between the collision partners,  $R$ , for three different angular momenta ( $l = 0, 1, 2$ ). The presence of a centrifugal barrier can be seen when  $l > 0$  (i.e., when the collision is not head-on). Right: schematic illustration depicting the influence of the impact parameter,  $b$ , on the outcome of a collision. As the solid lines indicate, there is no reaction when  $A^+$  and B collide at distances greater than  $b_{\text{max}}$ —the reactants are simply deflected by the ‘glancing’ collision. When  $b < b_{\text{max}}$ , the reactants are captured into a collision complex—indicated by the inward-spiraling lines, and resulting in a reaction event. From Zhang *et al.*, *Cold Chemistry: Molecular Scattering and Reactivity Near Absolute Zero*. Copyright 2018 The Royal Society of Chemistry. Reproduced with permission from The Royal Society of Chemistry.

short-range part of the potential that can influence the likelihood of a reaction proceeding to products, such as the presence of submerged barriers, also cannot be accounted for by capture theory models.<sup>2</sup> [It should, however, be noted that the strength of the attractive long-range forces frequently yields relatively fast ( $k > 10^{-11} \text{ cm}^3 \text{ s}^{-1}$ ) ion–neutral reaction rate coefficients in systems where submerged barriers are known to be present.]<sup>4</sup> Due to the non-inclusion of short-range interactions, and the assumption that all captured reactants go on to form products, capture theory methods are often seen as providing an upper limit of the reaction rate coefficient for a given system. Another limitation of capture theory methods is the treatment of molecules as point dipoles or point quadrupoles, meaning that predictions are less accurate for large polyatomic molecules.<sup>4</sup>

There have been several excellent review articles written that discuss different capture theory methods (see, for example, Refs. 3, 4, 6, and 7). Instead of simply summarizing and updating the work presented in these earlier articles, we aim to provide a fresh view on the topic. The goal of this Perspective is threefold: (i) to clearly communicate the strengths—and limitations—of capture theory predictions, through in-depth comparisons with experimental results, (ii) to assist in the selection of appropriate capture theory methods, for a given system and set of reaction conditions, and (iii) to identify the circumstances when capture theory predictions are most likely to be accurate. The article focuses on the most commonly used methods (including both classical and quantum approaches) adopted to describe ion–neutral reactions occurring at low temperatures.

The manuscript begins by outlining the theoretical development of capture-based approaches, from the early classical equations to the more rigorous quantum capture theory methods. The assumptions underpinning each of these approaches are provided, alongside the types of interactions that each method was developed to model. The strengths of the most widely used capture theory methods

are identified, followed by a discussion of the types of systems that capture theories cannot (yet) accurately account for. Finally, the impact that capture theories have had on our understanding of ion–molecule reactivity is discussed, with some possible future prospects for the field proposed.

### A. Classical capture theories

The simplest (and earliest) capture theory method is the Langevin equation. In the early 1900s, Langevin proposed a classical model to describe the interaction between ions and non-polar molecules.<sup>8,9</sup> Langevin rate coefficients can be calculated in SI units using

$$k_L = q \sqrt{\frac{\pi\alpha}{\epsilon_0\mu}}, \quad (4)$$

where  $\epsilon_0$  is the permittivity of free space and  $q$  is the ionic charge. The equation is derived assuming only the leading  $C_4/R^4$  contribution to the attractive potential is important [see Eq. (2)] and by determining the maximum value of the angular momentum  $l$  (and hence the maximum impact parameter, and cross section) for which the collision energy is above the barrier height. As indicated in Eq. (4), the model predicts a temperature independent rate coefficient for reactions between ions and non-polar molecules.

In ion–molecule reactions where the neutral species possesses a permanent dipole moment, Langevin theory is insufficient to describe the resulting long-range attraction that must include the leading  $C_2/R^2$  term. Subsequent capture theory methods sought to adapt the Langevin equation to include the effects of temperature, polarizability, dipole moment, and orientation of the reactants on the rate coefficient. One of the first such attempts was the ‘locked’

dipole (LD) orientation method.<sup>10</sup> The LD method assumes that the dipole of the polar molecule 'locks' at zero angle ( $\theta = 0$ ) when approaching the ion, yielding rate coefficients higher than those predicted by the Langevin model. Extending the LD method, average dipole orientation (ADO) theory suggests that the orientation of the dipole with respect to the ion can be treated as having an average value (rather than being permanently locked, as in the LD approach).<sup>11</sup> ADO reaction rate coefficients can be calculated in SI units using

$$k_{\text{ADO}} = q \sqrt{\frac{\pi\alpha}{\epsilon_0\mu}} + \frac{q\mu_{\text{DC}}}{\epsilon_0} \sqrt{\frac{1}{2\pi\mu k_{\text{B}} T}}, \quad (5)$$

where  $k_{\text{B}}$  is the Boltzmann constant and  $T$  is the temperature of the reaction system.

As can be seen in Eq. (5), the ADO model builds upon the Langevin equation by adding a term that accounts for the dipole moment and temperature dependence of the rate coefficient, giving rise to the inverse trend with temperature that has been observed experimentally in many ion–polar molecule reaction systems. The parameter  $c$  accounts for the average orientation of the dipole of the neutral reactant with respect to the ion ( $c = \cos\bar{\theta}$ ) and depends on both the ratio  $\mu_{\text{D}}/\alpha^{1/2}$  and the temperature of the system. While the ADO method was initially parameterized for ion–molecule reactions at 300 K, the authors extended the model to cover a wider temperature range (spanning 150–500 K) to facilitate more comparisons with experimental studies.<sup>12</sup> Note that when  $\bar{\theta} = 0$  and  $c = 1$ , the ADO equation becomes equivalent to the LD equation. To better account for the different types of interactions that can arise between ions and neutrals, two variations of the ADO model were subsequently developed: one that considers angular momentum conservation (AADO method) and one that includes quadrupole moment considerations (AQO model).<sup>13,14</sup>

The most widely used classical capture theory model for polar neutral reactants was developed by Su and Chesnavich (SC) in the early 1980s.<sup>15</sup> In the SC method, variational transition state theory and classical trajectory calculations are used to produce a set of trajectory curves, the empirical fit to which gives rise to reaction rate coefficients. The contribution of the dipole moment, polarizability, and temperature dependence is accounted for in the rate coefficient, introduced through a parameter,  $x$ , defined (in cgs-esu units) as

$$x = \frac{\mu_{\text{D}}}{\sqrt{2\alpha k_{\text{B}} T}}. \quad (6)$$

Depending on the value of  $x$ , the SC reaction rate coefficient ( $k_{\text{SC}}$ ) can be related to the Langevin rate coefficient ( $k_{\text{L}}$ ) for a given system at a selected  $T$ , as set out in the expressions

$$\frac{k_{\text{SC}}}{k_{\text{L}}} = 0.4767x + 0.6200, \quad x \geq 2 \quad (7)$$

and

$$\frac{k_{\text{SC}}}{k_{\text{L}}} = \frac{(x + 0.5090)^2}{10.526} + 0.9754, \quad x \leq 2. \quad (8)$$

Further details on how the trajectory calculations and benchmarking underpinning the SC method were carried out can be found in Ref. 15.

As with other classical capture theory models, SC predicts a negative trend with temperature. It is evident from Eqs. (4)–(8) that classical capture theory models are computationally straightforward to use. They were developed to approximate rate coefficients for ion–molecule reaction systems at temperatures near 300 K, as molecular species have a classical rotational distribution of states at such temperatures. At low temperatures, however, far fewer rotational states are occupied and classical capture theories start to break down. In Sec. I B, we introduce a number of more advanced, quantum capture theories, developed to account for low-temperature effects.

## B. Quantum capture theories

Quantum capture theories, such as the rotationally adiabatic capture theory proposed by Clary, take into account the contributions of individual rotational states of the neutral species to the likelihood of a reaction occurring.<sup>16</sup> For example, the adiabatic capture centrifugal sudden approximation (ACCSA) model was specifically developed for symmetric top neutral molecules and considers the quantum numbers ( $J, j, K, \Omega$ ) in the calculation, where  $J$  is the total angular momentum of the collisional pair,  $j$  the molecular (rotational) angular momentum of the neutral,  $K$  the projection of  $j$  onto the molecule-fixed axis, and  $\Omega$  the projection of  $J$  and  $j$  onto the body-fixed axis. (Using the centrifugal sudden approximation, couplings between different  $\Omega$  states can be neglected.) Rate coefficients for individual rotational states,  $k_{jK}$ , are calculated using

$$k_{jK}(T) = \sqrt{\frac{8}{\pi\mu(k_{\text{B}}T)^3}} \int_0^\infty \sigma(j, K, E) E \exp[-E/(k_{\text{B}}T)] dE, \quad (9)$$

where  $E$  is the collision energy and  $\sigma(j, K, E)$  is the state-specific reaction cross section. The reaction cross section can be calculated from the rotational adiabatic potential curves, produced by diagonalization of the relevant Hamiltonian, which includes molecular rotational, centrifugal, and interaction potential terms. In turn, the total ACCSA rate coefficient for a given  $T$  and distribution of rotational states can be calculated from

$$k_{\text{ACCSA}} = \frac{\sum_{jK} g_{jK} \exp[-E_{jK}/(k_{\text{B}}T)] k_{jK}(T)}{\sum_{jK} g_{jK} \exp[-E_{jK}/(k_{\text{B}}T)]}, \quad (10)$$

where  $g_{jK}$  is the degeneracy factor of a given state and  $E_{jK}$  is the barrier height of the corresponding potential curve. ACCSA predicts that lower rotational states have higher rate coefficients and that these state-selected rate coefficients increase with decreasing temperature. In their lowest rotational states, the alignment of the dipole moment of the polar molecule with the collision axis becomes more effective, enhancing the reaction rate. The ACCSA method has also been adapted for asymmetric top molecules.<sup>17,18</sup> Very recently, the ACCSA model was reformulated by considering the different Stark energies that polar molecules acquire as they approach the ionic reaction partner, rather than expressing that interaction in terms of multipole moments of the neutral species. Due to this internal Stark effect, the electric field induced by the ion lifts the degeneracy of the neutral's rotational states.<sup>19</sup> As will be discussed in Sec. II, this modification enabled ACCSA calculations to successfully describe experimental measurements undertaken at low collision energies.

Another quantum capture theory model that follows a similar approach to the ACCSA method is the statistical adiabatic channel model (SACM) developed by Troe.<sup>20</sup> SACM uses detailed analytical expressions to calculate state-selected and thermally averaged rate coefficients. Undertaking a comparison study between the SACM and the ACCSA models, the authors concluded that predictions from the two methods should yield equivalent results.<sup>20</sup> The SACM approach has been more extensively used to develop analytical results for effective potentials and rates (see, for example, Ref. 21) as opposed to the predominantly numerical calculations performed using the ACCSA method. Recent work has also seen the SACM approach adapted and applied to the study of inelastic and reactive collisions, with an alternative method of constructing the adiabatic potential curves introduced.<sup>22,23</sup>

It should be noted that rotationally adiabatic capture theory calculations, although not as straightforward as classical methods, are still considered to be (relatively) computationally easy to perform—especially when compared to the alternative of running *ab initio* calculations to construct potential energy surfaces (PESs) and the subsequent propagation of trajectories (either classical or quantum) on these surfaces.

While ACCSA and SACM are the most widely adopted quantum capture methods, other approaches have been developed. For example, the infinite-order sudden approximation (IOSA) uses the average behavior of the colliding reactants to establish the likelihood of a reaction occurring.<sup>24</sup> Rate coefficients and reaction cross sections are established for selected fixed orientation angles between the two collision partners and then averaged over all of these orientation angles. The IOSA approximation does not explicitly consider the contribution of different rotational states to the average rate coefficient. While the set of coupled IOSA equations is easy to use, the predictions are less accurate than those calculated from the rotationally adiabatic capture models.<sup>4</sup>

A different approach to calculating rate coefficients over a temperature range of 10–100 K was developed by Georgievskii and Klippenstein, with the long-range interactions modeled using variational transition state theory (TST).<sup>25</sup> Like many of the capture theory methods already introduced earlier, the long-range TST approach is based on the magnitude of the multipole moments of the reactants. As both energy and total angular momentum are conserved, the approach is best described as a microcanonical variational transition state theory ( $\mu$ J-VTST) implementation—yielding results that are effectively equivalent to the ACCSA and SACM methods. In all three cases, the Hamiltonian is diagonalized to yield a series of one-dimensional adiabatic interaction potentials, from which the rate coefficients can be obtained. (See Sec. 4.2.5 and Fig. 4.3 in Ref. 7 for a comparison between the predictions from SACM and long-range TST for the  $N^+ + H_2O$  reaction.)

Generally speaking, capture theory methods cannot predict reaction branching ratios (see discussion above). However, it is worth noting a special case where a rotationally adiabatic capture theory calculation was successfully adapted to measure the branching ratios of the different product channels for the  $O^+ + HD$  reaction systems. The hindered rotor wavefunction of the  $[OHD]^+$  complex was partitioned at the centrifugal barrier, and, subsequently, each partition was related to the different product species:  $OH^+ + D$  or  $OD^+ + H$ .<sup>26</sup> The branching ratio predictions were found to be in good agreement with experimental results, validating the

method.<sup>27</sup> Although this study was undertaken on a single reaction system with favorable properties, it demonstrates that it is possible for capture theory methods to predict channel-specific reaction rate coefficients.

### C. Full quantum capture theory for ultracold temperatures

The models described earlier all treat the translational motion along the reaction coordinate as classical, i.e., the collision energy is either high enough to pass over the centrifugal barrier with a probability of 1, or it is below the barrier height and the probability is zero. However, as the temperature is lowered well below 1 K, the de Broglie wavelength associated with this relative translation of the collision partners increases and becomes greater than the length scale of the potential barrier. Consequentially, the likelihood of tunneling and/or quantum reflection increases so that the classical model may become invalid. The ultracold region (often identified with temperatures below 1 mK) is also a regime in which the average angular momentum ( $l$ ) of successful collisions decreases, to the point where its quantization needs to be considered, making quantum effects such as tunneling and reflection more prominent. Furthermore, the adiabatic approximation discussed earlier may also be less valid at very low temperatures or collision energies.

In the full quantum version of capture theory, the classical ‘over the barrier’ model is replaced by a calculation of the penetration of a collisional wave past the barrier—the transmission probability. This wave is described as a superposition of partial waves with quantum number  $l$ , and even at energies below the barrier height for that  $l$  value, the transmission probability may be non-zero because of tunneling. Conversely, at energies above the barrier height, the transmission probability may be less than 1 because of the reflection that can occur when the wave meets the drop in the potential on the inner side of the barrier. In Fig. 3, the difference between the quantum and classical transmission probabilities is illustrated schematically.

The transmission probability can be determined by solving the Schrödinger equation for the scattering wave, and the adiabatic channel potentials are used to determine the effective barrier for the different  $l$  components and internal quantum states. The boundary conditions for the wave are set such that it has the form of an incoming scattering wave at long distance, with the colliding species in well-defined quantum states. At very short distances, an absorbing potential is applied such that the wave decays to zero near the repulsive inner wall of the potential.<sup>28</sup> The scattering wave can be expressed as a linear-combination of coupled channels, which allows the possibility of non-adiabatic transitions in the entrance channel between the adiabatic-channel states (i.e., there may be a change of quantum numbers as the reactants approach). The transmission probability is determined by the amplitude of the wave inside the barrier.

Full quantum capture theory calculations for the  $H_2 + H_2^+$  system were presented by Dashevskaya and co-workers<sup>29</sup> following their earlier presentation of the theory and a discussion about the temperature ranges where such calculations are needed.<sup>30</sup> As shown in Figs. 2 and 3 of Ref. 29, the reaction rate for  $H_2$  colliding in the  $J = 0$  state shows a small oscillation as a function of the collision

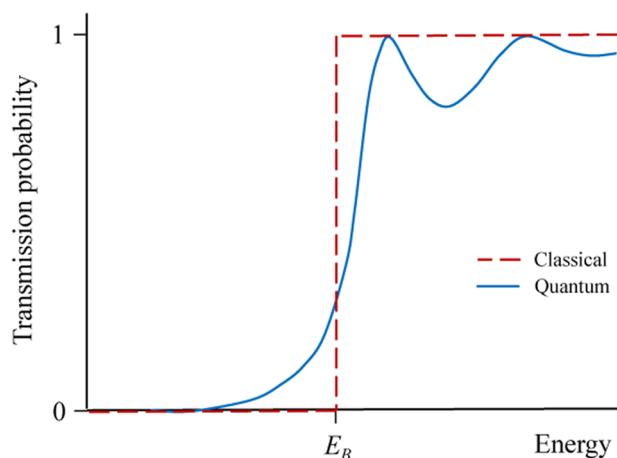


**FIG. 3.** The likelihood of a wave overcoming a barrier of height  $E_B$  is shown classically (red dashed line) and when considering the possibility of quantum effects (solid blue line). In the quantum model, the transmission probability is greater than zero at energies below  $E_B$  due to tunneling through the barrier, with the probability also below 1 at some energies above  $E_B$  due to quantum reflection (see main text). In contrast, the classical model appears as a step function: at all energies above  $E_B$ , the transmission probability is 1.

energy at collision energies of  $E_c/k_B \sim 1$  mK–10 K. The positions of the peaks in the oscillations are close to the classical threshold energies for the various partial waves  $l = 1, 2, 3, \dots$  and the form directly illustrates the contributions of tunneling and reflection in these partial-wave channels. At the lowest temperature (energy) of  $\leq 10^{-3}$  K, the rate shows a marked rise and converges to a zero-Kelvin limit equal to twice the temperature-independent Langevin rate coefficient. Only the  $s$ -wave component contributes to the rate at such low energies, and the centrifugal barrier does not exist for this component—this partial wave represents ‘head-on’ collisions with zero angular momentum. The zero-Kelvin limit is referred to as the Wigner–Bethe limit of pure quantum scattering.<sup>31</sup> At higher collision energies (above 100 mK), the oscillations in the calculated rate coefficient are smeared out and, eventually, there is convergence to the classical Langevin capture theory rate—hence, there is little need to use the full quantum capture theory at such temperatures. Similar results for the ‘Quantum Langevin’ system were reported by Gao,<sup>32</sup> and their methodology has been extended to a quantum defect theory approach to quantum scattering that allows prediction of some short-range effects, such as scattering resonances.<sup>33</sup>

Application of the full quantum capture theory to other molecular systems—with different masses, dipole moments, rotational constants, and polarizabilities—shows qualitatively similar behavior, but with the transition to pure  $s$ -wave scattering occurring at a different collision energy (temperature)—see Table 1 of Ref. 32. In most cases, the temperature is lower than for the  $\text{H}_2 + \text{H}_2^+$  system—typically in the micro-Kelvin or even nano-Kelvin regime. This is much lower than the temperatures at which ion–molecule collision rates have been measured to date, and hence the predicted quantum behavior has not been observed experimentally. However, recent merged-beam experiments (discussed in Sec. II)<sup>19,34</sup> point

to the possibility of entering this quantum regime, especially for low-mass collisional systems, such as  $\text{H}_2 + \text{H}_2^+$ .

## II. EXPERIMENTS AND APPLICATIONS

Section I focused on the theoretical development of capture theory methods, from the earliest classical models to the more in-depth quantum capture theories. To establish the accuracy of a given capture theory method, it is important to evaluate how well the method can account for the experimental observations it was developed to model. As set out earlier, the different capture theories were designed for different systems and different sets of experimental conditions. It is, therefore, unsurprising that different fields preferentially adopt certain methods. For example, the SC method is widely used in astrochemical modeling, whereas the ACCSA or SACM approaches are more frequently adopted by those wanting to understand state-selected reaction dynamics at low temperatures. Several of the experimental methods used to study ion–molecule reactions at temperatures below 300 K are described below. The role that each of these experimental techniques has played in validating, adapting, and challenging capture theory methods is set out in the following subsections. It is not the intention of this Perspective to assess the accuracy of capture theory predictions for every ion–molecule reaction system that has been studied at temperatures below 300 K. Instead, the following subsections strive to highlight key examples of ion–molecule reaction systems that have been studied using a variety of different experimental set-ups.

### A. Flow-based methods

#### 1. CRESU experiments

The CRESU technique—a French acronym standing for Cinétique de Réaction en Écoulement Supersonique Uniforme, or reaction kinetics in uniform supersonic flows—was developed in the early 1980s, alongside the development of a number of capture theories (as discussed in Sec. I). CRESU has been one of the leading techniques in low-temperature reaction studies, and, as such, early results from CRESU experiments played a key role in testing the validity of capture theory models. The technique takes advantage of the isentropic flows produced by a Laval nozzle to probe reactions within a supersonic beam at thermal equilibrium. Instead of presenting the extensive list of ion–molecule reactions studied using CRESU apparatus, this Perspective will focus on selected examples, including seminal studies for the establishment of capture theory models and reaction systems that show interesting behavior. A list of ion–molecule reaction studies undertaken using CRESU can be found in a number of recent review papers.<sup>35–38</sup>

One of the first experimental studies to test the validity of the classical Langevin theory at low temperatures was undertaken using the CRESU technique.<sup>39</sup> Reactions between  $\text{He}^+$  or  $\text{N}^+$  ions with a number of neutral species ( $\text{N}_2$ ,  $\text{O}_2$ ,  $\text{CO}$ , and  $\text{CH}_4$ ) were studied at temperatures as low as 8 K, achieving generally good agreement with classical capture theory predictions. Similarly, the reactions of  $\text{H}_3^+$  or  $\text{Ar}_2^+$  ions with a variety of neutral species (polar and non-polar) studied using CRESU further demonstrated the success of capture theories at describing the behavior of ion–molecule interactions at low temperatures.<sup>40,41</sup>

However, some early low-temperature experimental studies yielded results that did not agree with the reaction rate

coefficients predicted by capture theory methods, for example, CRESU studies of  $\text{He}^+$ ,  $\text{C}^+$ , or  $\text{N}^+$  ions with  $\text{H}_2\text{O}$  or  $\text{NH}_3$  at temperatures spanning 27–163 K.<sup>5</sup> While the expected negative temperature dependence was confirmed (as predicted from capture theory models), the rate coefficients for reactions involving  $\text{He}^+$  ions were suppressed in comparison with capture theory predictions. A subsequent theoretical study was undertaken to compare results of the  $\text{N}^+ + \text{H}_2\text{O}$  or  $\text{NH}_3$  systems with the ACCSA model (a seminal study for the establishment of the rotationally adiabatic capture theory model).<sup>17</sup> The ACCSA model was in excellent agreement with the  $\text{H}_2\text{O}$  findings; however, predictions for the  $\text{NH}_3$  system were found to be higher than the experimental results over the 27–163 K temperature range. [As an interesting aside, it was also noted that a measurement of the  $\text{N}^+ + \text{NH}_3$  reaction undertaken at 300 K using the selected ion flow tube (SIFT; see below) technique was in agreement with ACCSA predictions.] Further work—such as experimental studies conducted over a range of temperatures, or in-depth *ab initio* calculations—is required in order to explain the discrepancies between the experimental measurements and capture theory predictions.

Capture theory models were also unable to consistently predict rate coefficients for reactions between  $\text{N}^+$  ions and isomers of the  $\text{C}_2\text{H}_2\text{Cl}_2$  neutral.<sup>42</sup> The non-polar *trans*-1,2 isomer was found to react with a rate close to the Langevin prediction. However, the reactivity of the polar *cis*-1,2 and 1,1 isomers was suppressed in comparison with predictions from ACCSA calculations. A possible explanation for the disagreement between the measured and predicted rate coefficients was proposed, with the authors of the study speculating that the most favorable angle of approach of the polar isomers is not along the dipole axis (as is assumed within capture theory framework). Hence, if the approach is controlled by long-range forces to be along that axis, there will need to be short-range re-orientation for the reaction to occur.

Another study compared the ACCSA, SACM, and SC capture theory methods with experimental rate coefficients for the reactions of  $\text{He}^+$  or  $\text{C}^+$  ions with  $\text{HCl}$ ,  $\text{SO}_2$ , and  $\text{H}_2\text{S}$  molecules at temperatures spanning 27–300 K.<sup>43</sup> Excellent agreement was found between the CRESU results and capture theory predictions, with the exception of the  $\text{C}^+ + \text{HCl}$  system. A subsequent theoretical study was undertaken, looking more deeply at the parameters of the ACCSA model that are relevant for the  $\text{C}^+ + \text{HCl}$  reaction. Thanks to the findings from *ab initio* calculations, it was possible for additional details on the features of the PESs (such as the presence of multiple surfaces for this open shell system) to be included in an adapted form of the ACCSA model. This adapted ACCSA approach was able to successfully reproduce the experimental results.<sup>44</sup>

In several CRESU studies, including the  $\text{O}_2^+ + \text{CH}_4$  and  $\text{N}_2^+ + \text{O}_2$  reaction systems, reaction rate coefficients at 300 K were found to be suppressed in comparison with capture theory predictions.<sup>45,46</sup> However, rate coefficients displayed a strong increase with decreasing temperature, approaching the Langevin limit if extrapolated to 0 K. This behavior implies the formation of a long-lived intermediate complex—with the complex lifetime increasing as the temperature decreases, resulting in the observed enhanced reaction probability at lower temperatures (approaching the capture limit). Thus, it appears that the complex requires time to convert to products. In contrast, for the  $\text{O}^+ + \text{N}_2$  system, rate coefficients were found to remain two orders of magnitude lower than the Langevin limit at temperatures

spanning 23–300 K, with only a moderate negative temperature increase.<sup>47</sup>

A notably strong negative temperature dependence was observed for the  $\text{Cl}^- + \text{CH}_3\text{Br}$  system, with reaction rate coefficients (although suppressed in comparison to the SC model) increasing by two orders of magnitude as the temperature was decreased from 300 to 23 K.<sup>48</sup> *Ab initio* calculations identified a submerged barrier on the PES, just 2.9 kcal mol<sup>-1</sup> below the energy of the reactants. It was postulated that, at higher energies, the excited intermolecular bending modes of the transition state (modes that were not populated at low temperatures) effectively raise the height of the submerged barrier—such that it behaves like an energetic barrier to reaction, leading to the observed lower reaction probability.<sup>48</sup>

Recently, the importance of dipole–dipole interactions in ion–molecule systems was investigated in CRESU reactions between  $\text{HCOOH}$  neutrals and  $\text{CN}^-$  or  $\text{C}_3\text{N}^-$  anions. Calculations showed that the PESs of the  $\text{CN}^-$  and  $\text{C}_3\text{N}^-$  systems have a similar feature: a flat region close to the attractive wall. This so-called “reef” was proposed to slow down reactions at low temperatures.<sup>49</sup> However, very different dynamics were observed for the two systems when they were probed experimentally. The rate coefficient for  $\text{CN}^-$  anions exhibited no temperature dependence, deviating from the SC prediction at low temperatures (as expected from the features of the underlying PES). In contrast, the  $\text{C}_3\text{N}^-$  anions displayed a strong temperature dependence, in good agreement with the SC prediction. These findings were rationalized based on the different dipole moments of the anionic molecules;  $\text{C}_3\text{N}^-$  has a stronger dipole, and inclusion of the resulting strong ion–dipole–neutral–dipole forces enabled the SC method to successfully reproduce the experimental findings. The comparatively weaker dipole moment of  $\text{CN}^-$  meant that the short-range features of the PES exerted more influence over the rate coefficient. Reactions between  $\text{C}_3\text{N}^-$  or  $\text{CN}^-$  ions with a different neutral species,  $\text{HC}_3\text{N}$ , showed a similar behavior—with the former behaving as expected from ADO predictions, and the latter reacting slower than predicted by capture theory.<sup>50,51</sup>

## 2. SIFT and ICR studies

The selected ion flow tube (SIFT) technique and its subsequent adaptations such as SIFT-MS (mass spectrometry) and VISTA-SIFT (variable ion source temperature adjustable-SIFT) have been utilized since the 1970s to study a wide variety of ion–molecule reactions.<sup>52–54</sup> Using the SIFT technique, selected ionic species are inserted into a flowing carrier gas (enabling collisional thermalization of the ions), resulting in reactions with neutral species occurring at a selected position in the flow tube. Reaction products (or the depletion of reactants) are subsequently detected at the end of the flow tube using a quadrupole mass filter.<sup>52</sup> Over time, instrumental advances have retained the central reaction flow tube but have improved the selective nature of the source, as well as the efficiency of detection instruments.<sup>54</sup>

In a number of sub-300 K SIFT studies, especially those involving anions, the experimental rate coefficients were found to be significantly lower than the predicted Langevin rate coefficients. For example, the oxidation of  $\text{Al}_n^-$  clusters ( $3 \leq n \leq 17$ ) exhibited Arrhenius-like behavior, with a positive temperature dependence, due to the presence of an energetic barrier along the reaction coordinate (arising from the promotion of an electron from the Al

surface into the anti-bonding  $2\pi^*$  orbital of  $O_2$ ).<sup>54–56</sup> While other metallic cluster anions ( $V_n^-$ ,  $Cr_n^-$ ,  $Co_n^-$ , and  $Ni_n^-$ ) reacted faster than the Al anion clusters, with rate coefficients that were equal to or greater than Langevin capture rates, these cluster reactions all exhibited positive temperature dependencies. This led to the development of an adapted Arrhenius fit, incorporating the Langevin capture rate and a hard-sphere term into the pre-exponential factor. In this way, it was possible for an effective activation energy to be determined.<sup>54</sup>

Typically, capture theories are considered to provide an upper limit of the rate coefficient for ion–molecule systems (assuming an appropriate capture theory method has been selected, given the properties of the system). For the reactions of  $ArH_3^+$  with  $CO$ ,  $CH_4$ ,  $N_2$ , and  $O_2$  at 80 K, the experimental rate coefficients were found to exceed the capture prediction by a mean value of around 20%. [Langevin theory was used to predict the rate coefficients for non-polar neutrals ( $CH_4$ ,  $N_2$ , and  $O_2$ ), with ADO used for the polar neutral ( $CO$ ).]<sup>57</sup> Comparing the reactions of the same neutral species with  $H_3^+$  ions (instead of  $ArH_3^+$ ), under the same experimental conditions, yielded interesting results: all of the experimental rate coefficients were slightly smaller (within 2%, on average) than the capture prediction—aside from the reaction of  $H_3^+$  with  $O_2$ , where the experimental rate coefficient was considerably smaller than the Langevin prediction due to the presence of an endothermic proton transfer pathway.<sup>58</sup>

The unusual behavior of the  $ArH_3^+$  reactions, where the experimental rate coefficients were higher than predicted, was attributed to the large permanent dipole moment of  $ArH_3^+$  and the physical shape of the molecular ion giving rise to a larger capture cross section than was assumed within capture theory frameworks. As capture theories typically treat the ionic species as point charges, they do not always accurately model the reactions of ionic species with a significant dipole. Interactions of the ionic dipole with quadrupolar molecules ( $O_2$  and  $N_2$ ) are expected to account for the discrepancy between the experimental and Langevin rate coefficients in those systems—but  $CH_4$  does not have a quadrupole moment. Experimental rate coefficients that were higher than capture theory predictions were also observed in the reaction of  $ArH_3^+$  with some polar (including  $H_2O$  and  $NH_3$ ) and non-polar neutrals at 300 K.<sup>59</sup> ACCSA calculations were subsequently performed, with the inclusion of additional interactions to account for the properties of the  $ArH_3^+$  ion. Once these additional interactions were included in the modified ACCSA capture theory treatment, the predicted rate coefficients increased by  $\sim 18\%$  (for  $ArH_3^+ + H_2O$ ) and  $16\%$  (for  $ArH_3^+ + NH_3$ )—bringing them into agreement with the experimental measurements.<sup>60</sup>

In other cases, SIFT measurements (especially those involving cations) were in better agreement with appropriate capture theory predictions. A study investigating the reaction of  $H^+(H_2O)_n$  with  $CH_3CN$  reported reaction rate coefficients in agreement with ADO predictions over the temperature range 200–300 K.<sup>61</sup> The experimental rate coefficients for the reactions  $C^+ + NO$  and  $C^+ + O_2$  closely follow the ADO (for NO) or Langevin (for  $O_2$ ) theory predictions, for temperatures spanning 90–300 K.<sup>62</sup> Interestingly, the reaction of  $N^+ + CO$  was found to be well described by the ADO theory at 88 K, but as the temperature of the system increased the predicted and experimental rate coefficients deviated; at 454 K, the experimental

rate coefficient was only 50% of the predicted ADO capture rate coefficient.<sup>62</sup>

In several ion–neutral reaction systems where there are very few atoms involved (typically tri- or tetra-atomic systems), flow- and beam-based measurements have provided benchmark experimental data against which the accuracy of capture theory methods and quantum wave packet calculations have been assessed.<sup>63,64</sup> This can be seen in the  $O^+ + HD$  reaction, where the rotationally adiabatic capture method was adapted (as discussed in Sec. I B) to establish branching ratios and cross sections for the two product channels:  $OH^+ + D$  and  $OD^+ + H$ .<sup>26</sup> Subsequent experimental data, recorded in a guided ion beam apparatus at 105 K, were found to be in very good agreement with the adiabatic capture approximation predictions, suggesting that the features of the entrance channel (i.e., long-range effects) play a dominant role in dictating the outcome of a reactive collision.<sup>65</sup> More recently, the same system has been examined using state-to-state quantum wave packet calculations, spanning a range of astrochemically relevant temperatures.<sup>64</sup> Excellent agreement was found between the reaction cross sections established using wave packet calculations and those measured experimentally, as can be seen in Fig. 4. Thanks to the experimental validation of the theoretical findings, the calculated reaction properties were able to be confidently included in astrochemical models

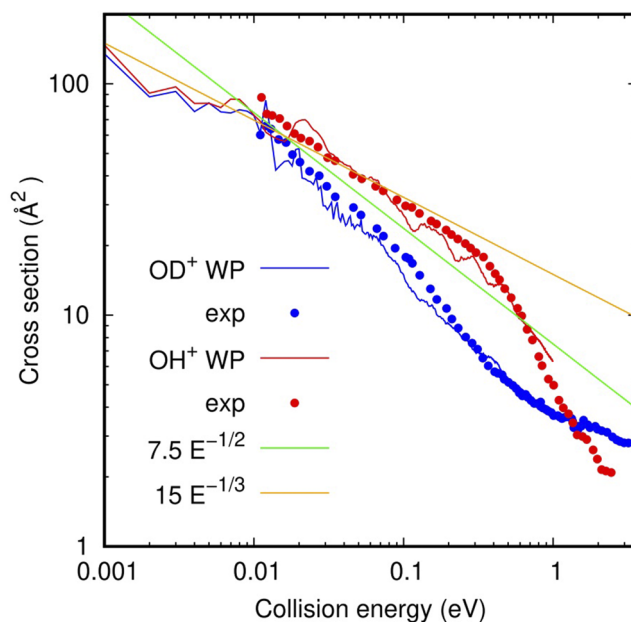


**FIG. 4.** Reaction cross sections are plotted as a function of collision energy for the  $O^+ + HD$  ( $v = 0, j = 0$ ) reaction, yielding  $OD^+$  or  $OH^+$  product ions. Experimental data from Sunderlin and Armentrout<sup>65</sup> are provided as blue and red dots, with the findings from quantum wave packet calculations included as solid blue and red lines. The trend predicted from a simple Langevin model, including charge-induced dipole long-range interactions (where the cross section scales with  $E^{-1/2}$ ), is shown in green. In yellow, the trend arising from a  $E^{-1/3}$  dependence of the cross section provides better agreement with the wave packet calculations at low collision energies. Figure reproduced with permission from Bulut *et al.*, *J. Phys. Chem. A* **124**, 6552 (2020). Copyright 2020, American Chemical Society.

to estimate the relative abundances of  $\text{OH}^+$  and  $\text{OD}^+$  in interstellar clouds.<sup>64</sup>

Ion cyclotron resonance (ICR) is a technique based on the use of a cylindrical Penning trap, which uses a combination of magnetic and electric fields to confine reactants. Reactions are detected mass spectrometrically by monitoring the cyclotron frequencies. Temperature-variable ICR set-ups have been used to study several collisions between ions and non-polar molecules, and in many cases, the experimental rate coefficients were greater than the Langevin predictions. For example, momentum transfer processes studied in  $\text{CH}_5^+ + \text{CH}_4$ ,  $\text{CF}_3^+ + \text{CF}_4$ , and  $\text{C}_4\text{H}_9^+ + \text{neo-C}_5\text{H}_{12}$  all exhibited rate coefficients greater than predicted by Langevin theory.<sup>66</sup> In the case of  $\text{CF}_3^+ + \text{CF}_4$ , while the ICR rate coefficients were largely independent of the temperature between 80 and 400 K (as expected for non-polar neutrals), they were consistently 20% higher than the Langevin prediction throughout this temperature range. To explain this behavior, it was proposed that the pure polarization potential—as assumed in the Langevin model—may not be sufficient to model the momentum transfer in the system. A model of the potential that included a repulsive interaction ( $r^{-12}$ ), an ion-induced quadrupole and dispersion interaction ( $r^{-6}$ ), and a long-range ion-induced dipole interaction ( $r^{-4}$ ), termed a 12-6-4 model, was found to better describe the properties of the system.<sup>67</sup> The need to include short-range interactions, in this case, implies that the position of the centrifugal barrier maximum occurs at quite short range.

## B. Trap-based methods

As highlighted in Sec. II A, flow techniques allow for the investigation of ion–molecule reactions under conditions of thermal equilibrium and over a wide temperature range. However, a caveat of flow-based methods, arising from the finite length of the flow tube, is that only relatively fast reactions can be studied. In contrast, ion traps can be used to confine ionic reactants for timescales of up to tens of minutes, or even hours, enabling slow processes to be studied. Radio frequency (RF) traps are most commonly used for reaction studies, with ions confined by a combination of static and alternating RF voltages applied to a number of cylindrical electrodes. It should be noted that the induced motion of the ions due to the RF oscillation means that the trapped species are not in thermal equilibrium.

### 1. 22-pole trap measurements

As already mentioned throughout this Perspective, low temperature experimental studies are necessary to test the validity of capture theory models developed to describe the behavior of different systems. A number of 22-pole trap set-ups have the ability to vary the reaction temperature from 300 K down to a few K, covering a range of atmospherically and astrochemically important conditions for gas-phase ion–molecule reactions. Temperatures are varied using techniques such as cryogenic cooling and buffer gas cooling for the ionic reactants, combined with (cooled or room temperature) effusive beams of neutrals.

Due to the key role hydrogen molecules play in the chemistry of the interstellar medium, with  $\text{H}_2$  the most abundant molecule in the universe, reactions between molecular hydrogen and ionic species have been extensively studied in 22-pole traps. A number of

selected examples will be discussed below. The  $\text{H}_3^+ + \text{HD}$  reaction system is thought to play a significant role in deuterium fractionation in the interstellar medium and has been studied at a temperature of 10 K.<sup>68</sup> Before there were such low temperature experimental measurements available, the rate coefficient for the reaction  $\text{H}_3^+ + \text{HD}$  in astrochemical databases was based on predictions from the Langevin model and extrapolated from SIFT measurements (undertaken at temperatures down to 80 K). Using a 22-pole trap, the rate coefficient was able to be experimentally measured at 10 K. Surprisingly, the rate coefficient for the forward reaction was significantly lower than the Langevin value, with the backward reaction being, instead, enhanced. Subsequent studies on the  $\text{H}_3^+ + \text{HD}$  reaction system, conducted under comparable conditions (in a cryogenic 22-pole trap environment), recorded a forward rate coefficient that was much closer to the Langevin prediction—and in good agreement with a microcanonical model.<sup>69</sup> Additional experimental and theoretical studies are required to resolve the discrepancy in the low-temperature experimental rate coefficients. Other 22-pole trap reaction studies at astrochemically relevant temperatures have posed similar challenges to the appropriateness of capture theory models for astrochemically relevant ion–molecule systems.<sup>70,71</sup>

As discussed earlier, the classical Langevin model predicts rate coefficients for reactions between ions and non-polar neutral species to be independent of temperature. Reaction studies undertaken using 22-pole traps have seen a number of examples where the Langevin model is insufficiently detailed to explain the behavior of ion–molecule systems as a function of temperature. For example, measurements on the reaction  $\text{C}_3^+ + \text{H}_2$  (or HD) found that rate coefficients increase with decreasing temperature, down to 50 K.<sup>72</sup> At 50 K, rate coefficients reach the Langevin limit and plateau at this value. The authors speculated that the suppression of rate coefficients at higher temperatures could be attributed to the decreased lifetime of the reaction complex (as discussed in other studies undertaken using the CRESU technique) or due to the excitation of bending modes at higher energies. It was noted that more accurate PESs and zero point energies are necessary to fully understand the behavior of the  $\text{C}_3^+ + \text{hydrogen}$  system. Similar findings were observed for the reaction systems  $\text{C}_3\text{H}^+ + \text{H}_2$  or HD and  $\text{OH}^+ + \text{D}_2$ .<sup>72,73</sup>

The proton transfer reactions between  $\text{NH}_2^-$  ions and  $\text{H}_2$  or  $\text{D}_2$  neutrals, studied at temperatures spanning 8–300 K, also featured rate coefficients that were suppressed compared to Langevin predictions.<sup>74</sup> However, instead of levelling off at low temperatures (as seen in the reactions discussed in the preceding paragraph), the rate coefficients “peaked” at around 20 K; reaction rate coefficients increased with decreasing temperature from 300 to 20 K, then decreased with decreasing temperature from 20 to 8 K. The disagreement with the Langevin model was more pronounced for the  $\text{D}_2$  neutrals. By combining calculations that use statistical theories of chemical reactivity (Rice–Ramsperger–Kassel–Marcus, RRKM, and phase-space theory, PST) with a scaled-down Langevin rate coefficient (in accordance with the experimentally measured rate coefficient at 300 K), the initial increase of the rate coefficients at temperatures spanning 300–100 K was reproduced for the  $\text{NH}_2^- + \text{H}_2$  system. However, at temperatures lower than 100 K the assumptions implicit in the RRKM and PST methods are no longer valid, resulting in deviations between the model and the experimental findings. As such, the low temperature behavior is yet to be fully accounted for.<sup>74</sup>

The few examples discussed earlier indicate that capture theory models alone (in particular, the classical Langevin model used in most 22-pole trap studies) cannot always account for the low-temperature behavior of ion–molecule reactions. When predictions are in disagreement with experimental findings, better agreement can often be achieved if the assumptions underlying the capture theory method of choice are specifically considered. For example, for associative detachment  $H^- + H$  reactions, at temperatures spanning 10–135 K, experimentally measured rate coefficients are enhanced when compared to Langevin predictions.<sup>75</sup> However, the experimental results are in good agreement with two theoretical models that more precisely model the long-range part of the interaction potential by accounting for a stronger polarization force (that is not considered in the Langevin model).<sup>76,77</sup>

## 2. Reaction studies in Coulomb crystals

The past few decades have seen the emergence of ion–neutral reaction studies within Coulomb crystals.<sup>78–86</sup> A Coulomb crystal can be formed when ions confined within a trap are laser cooled, resulting in the formation of an ordered lattice-like ('crystal') structure. Elastic collisions between the continuously laser-cooled ions and other co-trapped species enable multi-species Coulomb crystals to be generated. In this way, Coulomb crystals containing a diverse range of translationally cold ionic targets have been prepared. Experiments are conducted under ultra-high vacuum conditions, allowing processes to be monitored over an extended period of time. A number of complementary detection methods have been developed, with reaction rate coefficients and branching ratios reported for a number of ion–molecule reactions studied in Coulomb crystals.

In contrast to most of the flow-based measurements described earlier, the reactants in processes studied within Coulomb crystals are usually not in thermal equilibrium. (This is also the case for many other ion–neutral reaction studies monitored within ion traps.) The lack of equilibrium is a significant advantage for studies into the reaction dynamics, as it provides an opportunity to control and modify how energy is distributed in the reactants—and to independently study the importance of each of these reaction parameters. However, as thermal equilibrium is assumed to be present in many of the simpler capture theory methods, it is not always straightforward to apply these simpler models to reaction studies conducted in Coulomb crystals. For example, the widely used ADO method features a single temperature term to establish both the collision energy and the rotational energy of the polar molecule. As quantum capture theory methods enable the rotational state distribution of the neutral reactant to be specified independently of the collision energy, methods such as ACCSA and SACM are often used for the analysis of reactions conducted in Coulomb crystals.

A well-acknowledged challenge, as discussed throughout this Perspective, is predicting when the assumptions of capture theory apply to a given reaction system. Several charge–transfer reactions involving rare-gas ions and polar molecules have been also examined within Coulomb crystals over the past few years. In the reactions of three different rare-gas ions ( $Xe^+$ ,  $Kr^+$ , and  $Ar^+$ ) with ammonia (both  $NH_3$  and  $ND_3$ ), capture theory methods were unable to account for the observed rate coefficients, particularly their isotopic variation; both the ADO and ACCSA methods predicted rate coefficients that were significantly higher than what

was observed experimentally.<sup>87,88</sup> However, when the reactions of water ( $H_2O$  and  $D_2O$ ) isotopologues were studied with  $Kr^+$  ions, the experimental rate coefficients were in excellent agreement with predictions from capture theory, and the isotope effect was negligible.<sup>89</sup> From a capture theory perspective, one would expect the ammonia +  $Kr^+$  and water +  $Kr^+$  systems to exhibit very similar behavior: the dipole moment, polarizability, reduced mass, and collision energy are all very similar for the two systems—meaning that a classical capture theory (such as ADO) predicts that the two systems will behave in a very similar way. And yet, only one of these systems is well described by capture theory. In-depth *ab initio* calculations were able to identify a crossing point between the reactant and product PESs for the reaction of  $Kr^+$  with water, and the resulting charge transfer was found to be capture limited. In contrast, no energetically accessible crossing point was identified between the reactant and product surfaces for the charge transfer between ammonia and  $Kr^+$ , with charge transfer occurring more slowly than the capture limit.

In several other ion–molecule reaction systems studied within Coulomb crystals, experimental rate coefficients have been lower than predicted by capture theory—with this lower-than-capture-limit behavior attributed to the presence of features such as sub-merged barriers along the reaction coordinate. Such was the case for the reactions of ground-state  $Be^+$  ions with room-temperature  $H_2O$ ,<sup>90</sup> and for laser-cooled  $Ca^+$  ions with velocity-selected  $CH_3F$  or  $CH_3Cl$  reactants.<sup>2</sup> In other cases, the strength of non-adiabatic coupling between the reactant and product surfaces gave rise to state-dependent rate coefficients. For example, the interactions between long- and short-range forces were found to be dependent on the quantum state of the reactants in charge transfer reactions between ground- or excited-state Rb and sympathetically cooled  $O_2^+$  or  $N_2^+$  ions.<sup>91</sup> As no short-range effects or non-adiabatic coupling considerations are included in capture-based models, capture theory predictions could not account for the state-dependent behavior observed experimentally.

The reaction between velocity-filtered acetonitrile ( $CH_3CN$ ) and  $Ne^+$  ions was examined by monitoring the loss of  $Ne^+$  ions in a  $Ca^+$  Coulomb crystal as a function of time. Interestingly, the authors found that the perturbed rotational state (PRS) capture theory method was able to reproduce the experimental rate coefficient at low collision energies (<5 K), but that it could not account for the trend in the rate coefficient as a function of temperature.<sup>92</sup> The PRS method predicted a modest decrease of around 10%–20% in the rate coefficient as the collision energy was increased from 2 to 22 K, whereas the experimental rate coefficient decreased by 1.5 orders of magnitude over the same range.<sup>93</sup> As the authors of the study noted, further work is needed to establish why there is a deviation between capture theory predictions and the experimental measurements as the collision energy of the reactants is increased.

As noted earlier in the reaction of  $Kr^+$  with  $H_2O$  and  $D_2O$ , capture theory methods often do accurately predict the rate coefficients for ion–molecule reactions occurring within Coulomb crystals. For example, experimental measurements of the reaction between state-selected  $H_2O$  molecules and sympathetically cooled  $N_2H^+$  ions, yielding  $H_3O^+$  product ions, were in good agreement with predictions from rotationally adiabatic capture theory. The difference in the observed reactivity of two nuclear-spin iso-

mers of water (i.e., the different reactivity of molecules in the ground rotational state, *para*-water, and those in the first rotationally excited state, *ortho*-water) was able to be accounted for by considering the strength of the different ion–dipole interactions.<sup>94</sup> The cycloaddition reaction between 2,3-dibromo-1,3-butadiene ( $C_4H_4Br_2$ ) and propene ions ( $C_3H_6^+$ ) was studied using the same experimental set-up as for the  $H_2O + N_2H^+$  measurements. The experimentally measured conformer-specific rate coefficients were found to be in good agreement with predictions from rotationally adiabatic quantum capture theory: the centrifugally corrected long-range interaction potentials (including the ion–induced dipole and ion–permanent dipole considerations) determine the rate of reaction.<sup>95</sup> The agreement with capture theory for both isomers was surprising, given that one of the conformers is sterically disfavored to undergo the Diels Alder process in the expected concerted mechanism. However, *ab initio* calculation of the reaction pathways allowed for identification of the fast reaction route for both conformers.

Isotope-specific reactions between acetonitrile ( $CH_3CN$ ) and  $CCl^+$  ions were also examined within Coulomb crystals. Experimental rate coefficients were found to be in good general agreement with both ADO theory and RRKM-Master Equation (RRKM-ME) theoretical modeling, as can be seen in Fig. 5. PES calculations identified multiple pathways linking the reactants to possible products. All of the energetically accessible product channels were found to pass through the lowest-energy intermediate reaction complex (formed after the submerged barrier). The fast reaction was attributed to the low (submerged) barriers to isomerization (and ultimately product formation) along the reaction coordinate.<sup>96</sup> Note that ADO theory can only predict the total rate coefficient for product formation, whereas the RRKM-ME model can account for the branching between the two distinct product channels:  $HNCCI^+ + C_2H_2$ , and  $C_2H_3^+ + NCCL$ . At temperatures of around 300 K and above, rate coefficients from the RRKM-ME model were lower than those predicted by ADO theory, due to competition

from the reverse dissociation channel (i.e., not all captured reactants proceed to product formation at  $T \geq 300$  K, with some complexes dissociating back into reactants).<sup>96</sup> Finally, rate coefficients for reactions between non-polar neutral species and molecular ions [including  $CCl^+ + C_2H_2$  (acetylene),  $C_2D_2^+ + C_3H_4$  (hydrogenated allene), and  $C_2D_2^+ + C_3D_4$  (deuterated propyne)] were examined in Coulomb crystals, and were found to be consistent with Langevin predictions.<sup>97,98</sup>

### C. Methods that reach lower collision energies and other approaches

As discussed in Secs. II A and II B, experiments undertaken using flow- or trap-based techniques have played an important role in testing the validity of capture theory models at temperatures below 300 K. Only a handful of ion–molecule reactions have been studied at collision energies below 10 K, as realizing such low temperatures is experimentally challenging. One approach to achieving low collision energies is to merge the reactant beams, as seen in experiments using a Rydberg–Stark deflector where a Rydberg beam was merged with a neutral molecular beam at collision energies from 10 K down to a few hundred mK.<sup>99</sup> (Note that the ‘ionic’ reactants are formally neutral molecular species with an electron excited to a high Rydberg state; it is assumed that the Rydberg species reacts in the same way as the corresponding ionic species, with the Rydberg electron acting as a spectator.) For reactions between  $H_2^+$  ions and  $H_2$  neutrals, an enhancement of the rate coefficients was observed at temperatures below 1 K. Although the Langevin capture theory model predicts rate coefficients independent of the temperature for interactions between ions and non-polar molecules, excellent agreement was achieved between the experimental findings and an adapted version of the Langevin theory when the specific experimental parameters for this system were considered; after accounting for the ground *para*- $H_2$  and *ortho*- $H_2$  populations (25% and 75%, respectively), the experimental findings were successfully reproduced.<sup>29</sup>

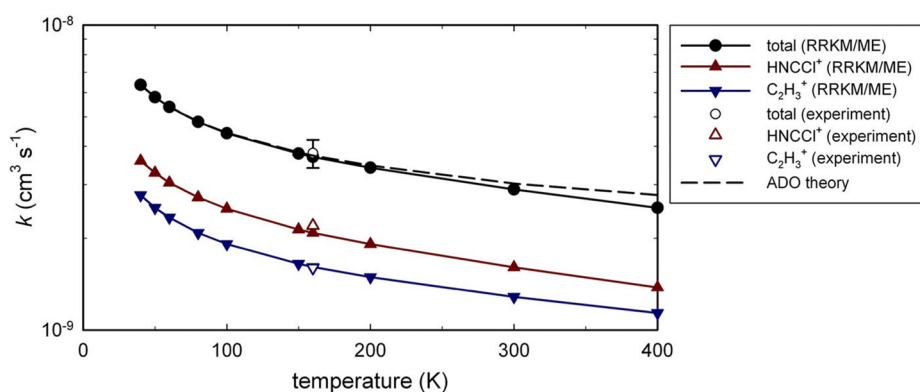


**FIG. 5.** Rate coefficients ( $k$ ) are plotted as a function of temperature for the reaction of  $CCl^+$  with  $CH_3CN$ . Each product channel is plotted separately, with  $HNCCI^+$  in red and  $C_2H_3^+$  in blue, for both the experimental (open points) and RRKM-ME (solid points and lines) rate coefficients, with the total rate coefficient for product formation provided in black. The ADO prediction—corresponding to the total rate coefficient (i.e., combining the contributions from the two product channels)—is plotted as a black dashed line. Figure reproduced with permission from Krohn *et al.*, *J. Chem. Phys.* **154**, 074305 (2021). Copyright 2021 AIP Publishing LLC.

Very recently, the same Rydberg–Stark deflector was used to study reactions between  $\text{He}^+$  and ammonia (both  $\text{NH}_3$  and  $\text{ND}_3$ ) at collision energies spanning 0–40 K.<sup>19</sup> A rotationally adiabatic capture theory method (based on the ACCSA and SACM models developed by Clary and Troe) successfully reproduced the experimental findings—accounting for the Stark shifts of the neutral rotational states induced by the ionic electric field. Furthermore, by considering the different nuclear spin statistics of the two isotopologues (and hence the different rotational level populations), the model was able to account for the observed enhanced rate coefficients of  $\text{ND}_3$  in comparison to  $\text{NH}_3$  at low collision energies. Using the same experimental approach for the  $\text{He}^+ + \text{N}_2$  reaction system, and including ion–quadrupole interactions in the capture theory modeling, the experimental measurements and predicted rate coefficients were again found to be in very good agreement.<sup>34</sup> A suppression of the rate coefficients was observed at collision energies below 10 K, with this behavior attributed to the negative quadrupole moment of the  $\text{N}_2$  reactant. Further calculations on  $\text{H}_2$  (a non-polar neutral with a positive quadrupole moment) confirmed the importance of the quadrupole moment, with a corresponding enhancement of the rate coefficient predicted at low collision energies.

A different merged beam apparatus uses a  $90^\circ$  deflector to direct a fast ion beam onto the axis of a fast neutral molecular beam, facilitating the study of ion–molecule reactions over a wide range of collision energies (from eV down to meV).<sup>100</sup> As the molecular ions are internally ‘hot’ (in some cases, reaching temperatures into the thousands of K), the systems studied using this apparatus are not in thermal equilibrium. Modifying capture theory models to account for this unequal distribution of energy in the system has seen the behavior of these ion–molecule reactions successfully described. In one example, the proton transfer reactions  $\text{C}(^3\text{P}) + \text{H}_2^+$  and  $\text{D}_2^+$  were studied at collision energies spanning 81–73110 K and 150–100960 K, respectively.<sup>101</sup> The experimentally measured cross sections at collision energies  $<0.1$  eV were compared with two capture theory models: the Langevin model and a more detailed capture model that accounts for the anisotropy of the  $\text{C}(^3\text{P})$  reactants as well as the influence of spin–orbit interactions on the interaction potentials. While both models were found to overestimate the experimentally measured cross sections, the more detailed method (with the inclusion of additional properties of the system) achieved better agreement at low collision energies.

While the techniques identified earlier include some of the most widely adopted methods for the study of ion–molecule reactions, they do not form an exhaustive list. For example, a number of ion–molecule reaction systems have been studied within helium nanodroplets. Due to the helium droplet environment—where there are frequent collisions with neighboring He atoms—reaction intermediates are collisionally cooled and can be trapped in local minima.<sup>102,103</sup> As such, the influence of the environment means that the central assumption of capture theory—that all captured reactants go on to form products—cannot be easily applied to these reactions. Other variations on the methods outlined earlier, such as the study of reactions within a ring electrode trap, have also been adopted,<sup>104</sup> with new techniques—and new combinations of existing techniques—continuing to emerge. More details on recent experimental developments in this field, and prospects for future set-ups, can be found in Refs. 85 and 105.

#### D. Wider applications of capture theories

Beyond predicting the likelihood of a reaction occurring when an ion and a neutral species collide, capture theories have also been applied to the study of three-body reaction systems. In a study on dimerization reactions involving ionic species and their neutral precursors, experimental results were compared with a theoretical analysis that assumed Langevin or ADO rate coefficients for the formation of the excited intermediate. The intermediate can subsequently collide with another neutral molecule, and this process can be described by a second rate coefficient (with the magnitude of the second rate coefficient scaled down, to account for the fact that not every collision between an excited complex and a neutral molecule results in stabilization of the complex; the complex can also dissociate back into the reactant species). In this way, overall rate coefficients for the dimerization reactions  $\text{CH}_2\text{CF}_2^+ + \text{CH}_2\text{CF}_2$ ,  $\text{C}_6\text{H}_6^+ + \text{C}_6\text{H}_6$ , and  $\text{C}_6\text{D}_6^+ + \text{C}_6\text{D}_6$  were formulated, in good agreement with the experimental rates of complex formation. However, it is interesting to note that, for example, the temperature dependencies of dimerization reactions involving benzene derivatives were not able to be described using this approach.<sup>106</sup>

### III. DISCUSSION

Generally speaking, an appropriate capture theory method can be selected to model the reactivity of a system when the long-range attractive forces that contribute to the interaction potential dominate the kinetics. This typically occurs in ion–molecule reactions that feature a direct pathway between the entrance channel and product formation, as can be seen in many of the reactions discussed in Sec. II. A key attraction of capture theory-based methods is their ease of use: armed with only a few properties of the reactants, rate coefficients can be straightforwardly predicted. As such, capture theory predictions are frequently included in databases of reactions that occur in complex gas-phase environments. For example, rate coefficients calculated using the SC method feature heavily in the Kinetic Database for Astrochemistry, KIDA.<sup>107</sup> In the absence of appropriate experimental measurements or high-level theoretical studies, capture theory predictions play a critical role in these databases; without a predicted value, numerous processes would otherwise be completely unaccounted for in the resulting chemical models. While including more experimental measurements is a long-acknowledged goal of the field—especially when it comes to properties such as branching ratios, which cannot be predicted from classical capture theory methods—kinetic databases are likely to rely on predicted rate coefficients for another few decades yet. In the absence of experimental data, it is not always obvious when long-range effects dominate or when a more in-depth treatment of the interaction potential (often requiring *ab initio* calculations) is needed to accurately describe the kinetics. Performing high-level *ab initio* calculations and constructing accurate full-dimensional PESs is not always feasible; it takes significant computational effort and time to undertake these calculations. Furthermore, many such studies involve open-shell ions, hence there may be multiple spin-states and multiple interacting PESs to calculate. So how can we anticipate when capture theory predictions are likely to be accurate?

In the first instance, treating capture theory predictions as an ‘upper limit’ of the experimental rate coefficient may be a useful approach. In the vast majority of the ion–molecule reaction systems we encountered when preparing this Perspective, capture theory predictions either agreed with or were higher than the experimental rate coefficient (assuming an appropriate capture theory method was selected). While counter examples do exist in the literature, as seen in the reactions of  $\text{ArH}_3^+$  above, this is often due to the simplified treatment of the ionic reactant as a point charge—with the effect disappearing when these interactions are accounted for. As such, selecting an appropriate capture theory method for the reaction system of interest is crucial to ensure that the assumptions underpinning the method are valid. When the reactants are non-polar, the Langevin model is often applicable (in some cases, with the addition of quadrupole moment considerations). In many of the reactions examined in this Perspective, where the reactants are polar molecules, the reaction conditions need to be considered more closely before selecting a capture theory method.

Under conditions where the system is at thermal equilibrium, the temperature is not too low (above  $\sim 150$  K), and when the spacing between the rotational energy levels is relatively small (i.e., when the rotational constants are small), then the classical capture methods, such as ADO or SC, are appropriate. When reactions occur at lower temperatures, or when considering molecules with a high  $B$ , only a few rotational states will be populated—making ACCSA or SACM more relevant. When there is unequal energy in the different degrees of freedom, then a method needs to be selected that defines the rotational energy and collision energy independently (as seen in variations of the SC method<sup>108</sup>). In the case of state-selected neutral reactants, a rotationally state-selected method (typically ACCSA or SACM) is required. As can be seen in recent studies using merged beams at collision energies down to  $<1$  K, it is sometimes necessary to extend or adapt an existing capture theory method to better describe the properties of the system and account for the experimental conditions.<sup>19,34</sup> Finally, as experiments approach ultracold temperatures, the full quantum version of capture theory will be required to properly account for the quantization of translational motion and to consider quantum effects, such as tunneling and reflection.

In cases where reactions proceed slower than predicted by the appropriate capture theory, this is usually due to the presence of important short-range effects. For example, reactants can fall into an intermediate complex well due to the presence of a submerged barrier along the reaction coordinate, or they can encounter an ‘inner’ transition state close to the exit channel.<sup>7</sup> The more time spent in this short-range part of the interaction potential, the more important these features become in influencing the rate of product formation. In general, greater complexity of the reagents leads to more complex reaction pathways, a multiplication of the number of degrees of freedom available to the reaction complex, and may increase the probability that the system does not proceed to reaction on the timescale of the complex. Short-range interactions are not typically included in the capture theory methods described earlier as they are challenging to accurately calculate—often requiring high-level *ab initio* electronic structure calculations. There are also more subtle considerations, such as systems where the centrifugal barrier is located at a shorter separation (as seen in reactions

involving H or  $\text{H}^+$ ), and may not be well described by long-range forces alone. Additional challenges can arise for reactions involving two open-shell reactants, as the reaction is unlikely to proceed along a single PES; multiple low-lying electronic states are often present, complicating the potential energy landscape.<sup>109</sup>

Theories have been proposed that can account for both long-range and short-range contributions to the interaction potential, such as the ‘two transition state model.’<sup>7</sup> While excellent agreement was achieved between the rate coefficients predicted by a two transition state model and those recorded in CRESU experimental studies, detailed *ab initio*-based transition state theory calculations were required. In some cases, however, detailed *ab initio* calculations and approaches such as the two transition state model are precisely what is required; adding more terms to the interaction potential cannot overcome the absence of short-range interactions in systems where short-range forces play an important role in the dynamics and kinetics.

#### IV. CONCLUSIONS

In conclusion, this Perspective has provided an overview of the different capture theory methods developed to describe reactions between ions and neutral molecules. Appropriate capture theory models have been identified for a range of reactants and experimental conditions. When an appropriate method is selected, capture theory predictions are likely to be accurate when two key criteria are met: (i) when the properties of the reactants are well accounted for by the model (i.e., when the interaction potential is accurately described and the assumptions underpinning the method are valid) and (ii) where there is a direct reaction pathway linking the reactants and the products (i.e., when the long-range attractive forces dominate the capture process). In cases where the short-range part of the interaction potential is important, such as when there are multiple nearby PESs or when the dynamics are not adiabatic, the capture theory prediction is likely to over-estimate the true rate coefficient. The development of more in-depth capture theory methods, alongside amendments to existing methods, has significantly expanded the range of systems and conditions that are amenable to capture theory modeling. Ion–molecule capture theory approaches have also influenced the development of models describing neutral–neutral interactions, in systems where long-range forces dominate the reaction process.<sup>7,110–112</sup> With continued developments in this field, the range of systems that can be described using capture-based models will increase and our understanding of the importance of the different forces at play will improve considerably.

#### ACKNOWLEDGMENTS

B.R.H. acknowledges the Engineering and Physical Sciences Research Council (EPSRC Project No. EP/N032950/2), the European Commission (ERC Starting Grant Project No. 948373), and the Community for Analytical and Measurement Science (CAMS fellowship) for funding.

#### AUTHOR DECLARATIONS

##### Conflict of Interest

The authors have no conflicts to disclose.

## Author Contributions

**Andriana Tsikritea:** Formal analysis (equal); Investigation (equal); Writing – original draft (equal); Writing – review & editing (equal). **Jake A. Diprose:** Investigation (equal); Writing – original draft (equal); Writing – review & editing (equal). **Timothy P. Softley:** Conceptualization (equal); Investigation (equal); Writing – original draft (equal); Writing – review & editing (equal). **Brianna R. Heazlewood:** Conceptualization (equal); Investigation (equal); Project administration (lead); Supervision (lead); Writing – original draft (equal); Writing – review & editing (equal).

## DATA AVAILABILITY

Data sharing is not applicable to this article as no new data were created or analyzed in this study.

## REFERENCES

- 1 S. Arrhenius, *Z. Phys. Chem.* **4U**, 96 (1889).
- 2 A. D. Gingell, M. T. Bell, J. M. Oldham, T. P. Softley, and J. N. Harvey, *J. Chem. Phys.* **133**, 194302 (2010).
- 3 D. Zhang and S. Willitsch, in *Cold Chemistry: Molecular Scattering and Reactivity Near Absolute Zero*, edited by A. Osterwalder and O. Dulieu (The Royal Society of Chemistry, 2018), pp. 496–536.
- 4 D. C. Clary, *Annu. Rev. Phys. Chem.* **41**, 61 (1990).
- 5 J. B. Marquette, B. R. Rowe, G. Dupeyrat, G. Poissant, and C. Rebrion, *Chem. Phys. Lett.* **122**, 431 (1985).
- 6 I. W. M. Smith, *Angew. Chem., Int. Ed.* **45**, 2842 (2006).
- 7 S. J. Klippenstein and Y. Georgievskii, in *Low Temperatures and Cold Molecules*, edited by I. W. M. Smith (Imperial College Press, London, 2008), pp. 175–229.
- 8 M. P. Langevin, *Ann. Chim. Phys.* **5**, 245–288 (1905).
- 9 G. Gioumousis and D. P. Stevenson, *J. Chem. Phys.* **29**, 294 (1958).
- 10 T. F. Moran and W. H. Hamill, *J. Chem. Phys.* **39**, 1413 (1963).
- 11 T. Su and M. T. Bowers, *J. Chem. Phys.* **58**, 3027 (1973).
- 12 T. Su and M. T. Bowers, *Int. J. Mass Spectrom. Ion Processes* **17**, 211 (1975).
- 13 T. Su, E. C. F. Su, and M. T. Bowers, *J. Chem. Phys.* **69**, 2243 (1978).
- 14 T. Su and M. T. Bowers, *Int. J. Mass Spectrom. Ion Phys.* **17**, 309 (1975).
- 15 T. Su and W. J. Chesnavich, *J. Chem. Phys.* **76**, 5183 (1982).
- 16 D. C. Clary, *Mol. Phys.* **54**, 605 (1985).
- 17 D. C. Clary, *J. Chem. Soc., Faraday Trans. 2* **83**, 139 (1987).
- 18 T. Stoecklin, D. C. Clary, and A. Palma, *J. Chem. Soc., Faraday Trans.* **88**, 901 (1992).
- 19 V. Zhelyazkova, F. B. V. Martins, J. A. Agner, H. Schmutz, and F. Merkt, *Phys. Chem. Chem. Phys.* **23**, 21606 (2021).
- 20 J. Troe, *J. Chem. Phys.* **87**, 2773 (1987).
- 21 J. Troe, *J. Chem. Phys.* **105**, 6249 (1996).
- 22 M. Konings, B. Desrousseaux, F. Lique, and J. Loreau, *J. Chem. Phys.* **155**, 104302 (2021).
- 23 J. Loreau, F. Lique, and A. Faure, *Astrophys. J., Lett.* **853**, L5 (2018).
- 24 R. T. Pack, *J. Chem. Phys.* **60**, 633 (1974).
- 25 Y. Georgievskii and S. J. Klippenstein, *J. Chem. Phys.* **122**, 194103 (2005).
- 26 C. E. Dateo and D. C. Clary, *J. Chem. Soc., Faraday Trans. 2* **85**, 1685 (1989).
- 27 J. D. Burley, K. M. Ervin, and P. B. Armentrout, *Int. J. Mass Spectrom. Ion Processes* **80**, 153 (1987).
- 28 E. J. Rackham, T. Gonzalez-Lezana, and D. E. Manolopoulos, *J. Chem. Phys.* **119**, 12895 (2003).
- 29 E. I. Dashevskaya, I. Litvin, E. E. Nikitin, and J. Troe, *J. Chem. Phys.* **145**, 244315 (2016).
- 30 E. E. Nikitin and J. Troe, *Phys. Chem. Chem. Phys.* **7**, 1540 (2005).
- 31 E. I. Dashevskaya, A. I. Maergoiz, J. Troe, I. Litvin, and E. E. Nikitin, *J. Chem. Phys.* **118**, 7313 (2003).
- 32 B. Gao, *Phys. Rev. A* **83**, 062712 (2011).
- 33 B. Gao, *arXiv:2008.08018* (2020).
- 34 V. Zhelyazkova, F. B. V. Martins, M. Žeško, and F. Merkt, *Phys. Chem. Chem. Phys.* **24**, 2843 (2022).
- 35 I. R. Cooke and I. R. Sims, *ACS Earth Space Chem.* **3**, 1109 (2019).
- 36 A. Potapov, A. Canosa, E. Jiménez, and B. Rowe, *Angew. Chem., Int. Ed.* **56**, 8618 (2017).
- 37 I. W. M. Smith and B. R. Rowe, *Acc. Chem. Res.* **33**, 261 (2000).
- 38 A. Canosa, F. Goulay, I. R. Sims, and B. R. Rowe, in *Low Temperatures and Cold Molecules*, edited by I. W. M. Smith (Imperial College Press, London, 2008), pp. 55–120.
- 39 B. R. Rowe, J. B. Marquette, G. Dupeyrat, and E. E. Ferguson, *Chem. Phys. Lett.* **113**, 403 (1985), available at <https://adsabs.harvard.edu/pdf/1989A%26A...213L..29M>
- 40 J. B. Marquette, C. Rebrion, and B. R. Rowe, *Astron. Astrophys.* **213**, L29 (1989).
- 41 G. Dupeyrat, J. B. Marquette, B. R. Rowe, and C. Rebrion, *Int. J. Mass Spectrom. Ion Processes* **103**, 149 (1991).
- 42 C. Rebrion, J. B. Marquette, B. R. Rowe, C. Chakravarty, D. C. Clary, N. G. Adams, and D. Smith, *J. Phys. Chem.* **92**, 6572 (1988).
- 43 C. Rebrion, J. B. Marquette, B. R. Rowe, and D. C. Clary, *Chem. Phys. Lett.* **143**, 130 (1988).
- 44 C. E. Dateo and D. C. Clary, *J. Chem. Phys.* **90**, 7216 (1989).
- 45 B. R. Rowe, G. Dupeyrat, J. B. Marquette, D. Smith, N. G. Adams, and E. E. Ferguson, *J. Chem. Phys.* **80**, 241 (1984).
- 46 P. Gaucherel, J. B. Marquette, C. Rebrion, G. Poissant, G. Dupeyrat, and B. R. Rowe, *Chem. Phys. Lett.* **132**, 63 (1986).
- 47 J.-L. Le Garrec, S. Carles, T. Speck, J. B. A. Mitchell, B. R. Rowe, and E. E. Ferguson, *Chem. Phys. Lett.* **372**, 485 (2003).
- 48 J.-L. Le Garrec, B. R. Rowe, J. L. Queffelec, J. B. A. Mitchell, and D. C. Clary, *J. Chem. Phys.* **107**, 1021 (1997).
- 49 B. Joalland, N. Jamal-Eddine, J. Klos, F. Lique, Y. Trolez, J.-C. Guillemin, S. Carles, and L. Biennier, *J. Phys. Chem. Lett.* **7**, 2957 (2016).
- 50 L. Biennier, S. Carles, D. Cordier, J.-C. Guillemin, S. D. Le Picard, and A. Faure, *Icarus* **227**, 123 (2014).
- 51 J. Bourgalais, N. Jamal-Eddine, B. Joalland, M. Capron, M. Balaganesh, J.-C. Guillemin, S. D. Le Picard, A. Faure, S. Carles, and L. Biennier, *Icarus* **271**, 194 (2016).
- 52 N. G. Adams and D. Smith, *Int. J. Mass Spectrom. Ion Phys.* **21**, 349 (1976).
- 53 D. Smith and P. Španěl, *Mass Spectrom. Rev.* **24**, 661 (2005).
- 54 S. G. Ard, A. A. Viggiano, and N. S. Shuman, *J. Phys. Chem. A* **125**, 3503 (2021).
- 55 R. Yin, Y. Zhang, F. Libisch, E. A. Carter, H. Guo, and B. Jiang, *J. Phys. Chem. Lett.* **9**, 3271 (2018).
- 56 F. Libisch, C. Huang, P. Liao, M. Pavone, and E. A. Carter, *Phys. Rev. Lett.* **109**, 198303 (2012).
- 57 D. Smith, P. Španěl, and D. K. Bedford, *Chem. Phys. Lett.* **191**, 587 (1992).
- 58 N. G. Adams and D. Smith, *Chem. Phys. Lett.* **105**, 604 (1984).
- 59 C. Praxmarer, A. Hansel, and W. Lindinger, *J. Chem. Phys.* **100**, 8884 (1994).
- 60 D. C. Clary, *Chem. Phys. Lett.* **232**, 267 (1995).
- 61 D. Smith, N. G. Adams, and E. Alge, *Planet. Space Sci.* **29**, 449 (1981).
- 62 T. M. Miller, R. E. Wetterskog, and J. F. Paulson, *J. Chem. Phys.* **80**, 4922 (1984).
- 63 S. Gómez-Carrasco, B. Godard, F. Lique, N. Bulut, J. Klos, O. Roncero, A. Aguado, F. J. Aoiz, J. F. Castillo, J. R. Goicoechea *et al.*, *Astrophys. J.* **794**, 33 (2014).
- 64 N. Bulut, O. Roncero, and F. Lique, *J. Phys. Chem. A* **124**, 6552 (2020).
- 65 L. S. Sunderlin and P. B. Armentrout, *Chem. Phys. Lett.* **167**, 188 (1990).
- 66 M. T. Bowers, P. V. Neilson, P. R. Kemper, and A. G. Wren, *Int. J. Mass Spectrom. Ion Phys.* **25**, 103 (1977).
- 67 D. P. Ridge and J. L. Beauchamp, *J. Chem. Phys.* **64**, 2735 (1976).
- 68 D. Gerlich, E. Herbst, and E. Roueff, *Planet. Space Sci.* **50**, 1275 (2002).
- 69 E. Hugo, O. Asvany, and S. Schlemmer, *J. Chem. Phys.* **130**, 164302 (2009).
- 70 T. D. Tran, S. Rednyk, A. Kovalenko, Š. Roučka, P. Dohnal, R. Plašil, D. Gerlich, and J. Glosík, *Astrophys. J.* **854**, 25 (2018).

- <sup>71</sup>R. Plašil, S. Rednyk, A. Kovalenko, T. D. Tran, Š. Roučka, P. Dohnal, O. Novotný, and J. Glosík, *Astrophys. J.* **910**, 155 (2021).
- <sup>72</sup>I. Savić and D. Gerlich, *Phys. Chem. Chem. Phys.* **7**, 1026 (2005).
- <sup>73</sup>D. Mulin, Š. Roučka, P. Jusko, I. Zymak, R. Plašil, D. Gerlich, R. Wester, and J. Glosík, *Phys. Chem. Chem. Phys.* **17**, 8732 (2015).
- <sup>74</sup>R. Otto, J. Mikosch, S. Trippel, M. Weidemüller, and R. Wester, *Phys. Rev. Lett.* **101**, 063201 (2008).
- <sup>75</sup>D. Gerlich, P. Jusko, Š. Roučka, I. Zymak, R. Plašil, and J. Glosík, *Astrophys. J.* **749**, 22 (2012).
- <sup>76</sup>M. Cížek, J. Horáček, and W. Domcke, *J. Phys. B: At., Mol. Opt. Phys.* **31**, 2571 (1998).
- <sup>77</sup>K. Sakimoto, *Chem. Phys. Lett.* **164**, 294 (1989).
- <sup>78</sup>K. Mølhave and M. Drewsen, *Phys. Rev. A* **62**, 011401(R) (2000).
- <sup>79</sup>S. Willitsch, M. T. Bell, A. D. Gingell, and T. P. Softley, *Phys. Chem. Chem. Phys.* **10**, 7200 (2008).
- <sup>80</sup>M. T. Bell, A. D. Gingell, J. M. Oldham, T. P. Softley, and S. Willitsch, *Faraday Discuss.* **142**, 73 (2009).
- <sup>81</sup>S. Willitsch, *Int. Rev. Phys. Chem.* **31**, 175 (2012).
- <sup>82</sup>B. R. Heazlewood and T. P. Softley, *Annu. Rev. Phys. Chem.* **66**, 475 (2015).
- <sup>83</sup>R. C. Thompson, *Contemp. Phys.* **56**, 63 (2015).
- <sup>84</sup>B. R. Heazlewood, *Mol. Phys.* **117**, 1934 (2019).
- <sup>85</sup>J. Toscano, H. J. Lewandowski, and B. R. Heazlewood, *Phys. Chem. Chem. Phys.* **22**, 9180 (2020).
- <sup>86</sup>B. R. Heazlewood and H. J. Lewandowski, in *Emerging Trends in Chemical Applications of Lasers* (ACS Publications, 2021), pp. 389–410.
- <sup>87</sup>L. S. Petralia, A. Tsikritea, J. Loreau, T. P. Softley, and B. R. Heazlewood, *Nat. Commun.* **11**, 173 (2020).
- <sup>88</sup>A. Tsikritea, K. Park, P. Bertier, J. Loreau, T. P. Softley, and B. R. Heazlewood, *Chem. Sci.* **12**, 10005 (2021).
- <sup>89</sup>A. Tsikritea, J. A. Diprose, J. Loreau, and B. R. Heazlewood, *ACS Phys. Chem. Au* **2**, 199 (2022).
- <sup>90</sup>T. Yang, A. Li, G. K. Chen, C. Xie, A. G. Suits, W. C. Campbell, H. Guo, and E. R. Hudson, *J. Phys. Chem. Lett.* **9**, 3555 (2018).
- <sup>91</sup>A. D. Dörfler, P. Eberle, D. Koner, M. Tomza, M. Meuwly, and S. Willitsch, *Nat. Commun.* **10**, 5429 (2019).
- <sup>92</sup>K. Takayanagi, *J. Phys. Soc. Jpn.* **45**, 976 (1978).
- <sup>93</sup>K. Okada, K. Sakimoto, Y. Takada, and H. A. Schuessler, *J. Chem. Phys.* **153**, 124305 (2020).
- <sup>94</sup>A. Kilaj, H. Gao, D. Rösch, U. Rivero, J. Küpper, and S. Willitsch, *Nat. Commun.* **9**, 2096 (2018).
- <sup>95</sup>A. Kilaj, J. Wang, P. Straňák, M. Schwilk, U. Rivero, L. Xu, O. A. von Lilienfeld, J. Küpper, and S. Willitsch, *Nat. Commun.* **12**, 6047 (2021).
- <sup>96</sup>O. A. Krohn, K. J. Catani, J. Greenberg, S. P. Sundar, G. da Silva, and H. J. Lewandowski, *J. Chem. Phys.* **154**, 074305 (2021).
- <sup>97</sup>P. C. Schmid, J. Greenberg, T. L. Nguyen, J. H. Thorpe, K. J. Catani, O. A. Krohn, M. I. Miller, J. F. Stanton, and H. J. Lewandowski, *Phys. Chem. Chem. Phys.* **22**, 20303 (2020).
- <sup>98</sup>K. J. Catani, J. Greenberg, B. V. Saarel, and H. J. Lewandowski, *J. Chem. Phys.* **152**, 234310 (2020).
- <sup>99</sup>P. Allmendinger, J. Deiglmayr, K. Höveler, O. Schullian, and F. Merkt, *J. Chem. Phys.* **145**, 244316 (2016).
- <sup>100</sup>A. P. O'Connor, X. Urbain, J. Stützel, K. A. Miller, N. de Ruette, M. Garrido, and D. W. Savin, *Astrophys. J., Suppl. Ser.* **219**, 6 (2015).
- <sup>101</sup>P.-M. Hillenbrand, K. P. Bowen, F. Dayou, K. A. Miller, N. de Ruette, X. Urbain, and D. W. Savin, *Phys. Chem. Chem. Phys.* **22**, 27364 (2020).
- <sup>102</sup>A. Mauracher, O. Echt, A. M. Ellis, S. Yang, D. K. Bohme, J. Postler, A. Kaiser, S. Denifl, and P. Scheier, *Phys. Rep.* **751**, 1 (2018).
- <sup>103</sup>M. Fárník and J. P. Toennies, *J. Chem. Phys.* **122**, 014307 (2005).
- <sup>104</sup>B. Yuan, Z. Scott, G. Tikhonov, D. Gerlich, and M. A. Smith, *J. Phys. Chem. A* **115**, 25 (2011).
- <sup>105</sup>B. R. Heazlewood and T. P. Softley, *Nat. Rev. Chem.* **5**, 125 (2021).
- <sup>106</sup>S. Liu, M. F. Jarrold, and M. T. Bowers, *J. Phys. Chem.* **89**, 3127 (1985).
- <sup>107</sup>V. Wakelam, E. Herbst, J.-C. Loison, I. W. M. Smith, V. Chandrasekaran, B. Pavone, N. G. Adams, M.-C. Bacchus-Montabonel, A. Bergeat, K. Béroff *et al.*, *Astrophys. J., Suppl. Ser.* **199**, 21 (2012).
- <sup>108</sup>T. Su, *J. Chem. Phys.* **100**, 4703 (1994).
- <sup>109</sup>L. Y. Wu, C. Miossec, and B. R. Heazlewood, *Chem. Commun.* **58**, 3240 (2022).
- <sup>110</sup>T. Stoeklin, C. E. Dateo, and D. C. Clary, *J. Chem. Soc., Faraday Trans.* **87**, 1667 (1991).
- <sup>111</sup>M. Auzinsh, E. I. Dashevskaya, I. Litvin, E. E. Nikitin, and J. Troe, *J. Phys. Chem. A* **115**, 5027 (2011).
- <sup>112</sup>M. Lepers and O. Dulieu, in *Cold Chemistry: Molecular Scattering and Reactivity Near Absolute Zero*, edited by A. Osterwalder and O. Dulieu (The Royal Society of Chemistry, 2018), pp. 150–202.